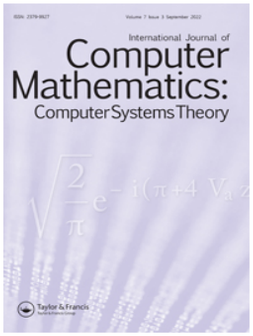

International Journal of Computer Mathematics: Computer Systems Theory

ISSN: (Print) (Online) Journal homepage: https://www.tandfonline.com/loi/tcom20

Nonlocal diffusion of variable order on complex networks

Daniele Bertaccini & F. Durastante

To cite this article: Daniele Bertaccini & F. Durastante (2022) Nonlocal diffusion of variable order on complex networks, International Journal of Computer Mathematics: Computer Systems Theory, 7:3, 172-191, DOI: 10.1080/23799927.2022.2114381

To link to this article: https://doi.org/10.1080/23799927.2022.2114381

Published online: 13 Sep 2022.

INTERNATIONAL JOURNAL OF COMPUTER MATHEMATICS: COMPUTER SYSTEMS THEORY
2022, VOL. 7, NO. 3, 172–191
https://doi.org/10.1080/23799927.2022.2114381

Nonlocal diffusion of variable order on complex networks

Daniele Bertaccini[a,b] and F. Durastante[c]

[a]Dipartimento di Matematica, Università di Roma Tor Vergata, Roma, Italy; [b]Consiglio Nazionale delle Ricerche, Istituto per le Applicazioni del Calcolo 'M. Picone', Roma, Italy; [c]Dipartimento di Matematica, Università di Pisa, Pisa, Italy

ABSTRACT

Some aspects of nonlocal dynamics on directed and undirected networks for an initial value problem whose Jacobian matrix is a variable-order fractional power of a Laplacian matrix are discussed here. This is a new extension to non-stationary behaviour of a class of non-local phenomena on complex networks for which both directed and undirected graphs are considered. Under appropriate assumptions, the existence, uniqueness, and uniform asymptotic stability of the solutions of the underlying initial value problem are proved. Some examples giving a sample of the behaviour of the dynamics are also included.

ARTICLE HISTORY
Received 29 November 2021
Revised 13 July 2022
Accepted 22 July 2022

KEYWORDS
Network dynamics; nonlocal dynamics; superdiffusion

1. Introduction

To model the evolution of probability distributions on graphs, two popular approaches are represented by the heat equation

$$\begin{cases} \mathbf{p}'(t) = -\mathbf{p}(t)J, & t > 0, \\ \mathbf{p}(0) = \mathbf{p}_0, & \sum_{j=1}^{n} (\mathbf{p}_0)_j = 1, \end{cases} \tag{1}$$

and by the Schrödinger equation

$$\begin{cases} \boldsymbol{\psi}'(t) = -i\,\boldsymbol{\psi}(t)J, & t > 0, \\ \boldsymbol{\psi}(0) = \boldsymbol{\psi}_0, & \sum_{j=1}^{n} |(\boldsymbol{\psi}_0)_j|^2 = 1, \end{cases} \tag{2}$$

where $\mathbf{p}(t) \geq 0$ is a time-dependent probability distribution in (1), and, in (2), the probability that a particle at time t is at node $v_j \in V$, V the set of all the nodes, is $|\psi_j(t)|^2 / \sum_{j=1}^{n} |\psi_j(t)|^2$. The matrix J is usually the combinatorial Laplacian matrix L associated to the graph $G = (V, E)$ and is related to adjacency and degree matrices A and D, i.e. the singular M-matrix

$$L = D - A, \quad D = \operatorname{diag}(A\mathbf{1}), \quad (A)_{l,j} = a_{l,j} = \begin{cases} 1, & (v_l, v_j) \in E, \\ 0, & \text{otherwise.} \end{cases} \tag{3}$$

The solutions of Equations (1) and (2) produce a probability distribution/density at each time step t, with the caveat that for (2) we need to consider the amplitudes $|\psi_j(t)|^2$, $j = 1, \ldots, n$, and model

CONTACT Daniele Bertaccini bertaccini@mat.uniroma2.it

the evolution of the probability distribution for a random walker on G that moves between adjacent nodes, that is locally. Recently, there has been an interest in expanding these navigational strategies to cover also the evolution of probability distributions on G for walkers that perform 'long jumps', i.e. Lévy flights, on the underlying graph. To achieve this result, generalizations of (1) and (2) in which the combinatorial Laplacian matrix is substituted by either its fractional power L^α, $\alpha \in (0, 1]$, have been proposed; see [6,33,34], or by the generalized k-path Laplacian matrix L_G; see [17,20,21]. In both cases, the choice of the type of jumps we want our walker to perform on G are selected to be the same for all times t, while it could be more natural to think about a walker following non-stationary jumps instead. Sometimes, it can decide to explore the network locally, some others its attention span is diminished and opts to start skipping the nodes by performing longer jumps. To model this behaviour, we consider the nonautonomous extensions of (1) and (2) given by

$$\begin{cases} \mathbf{p}'(t) = -\mathbf{p}(t)\mathcal{L}(t), & t > 0, \\ \mathbf{p}(0) = \mathbf{p}_0, \end{cases} \qquad \begin{cases} \boldsymbol{\psi}'(t) = -i\,\boldsymbol{\psi}(t)\mathcal{L}(t), & t > 0, \\ \boldsymbol{\psi}(0) = \boldsymbol{\psi}_0, \end{cases} \tag{4}$$

where $\mathbf{p}(t) \geq 0$ is a time-dependent probability distribution, the amplitudes associated with $\boldsymbol{\psi}(t)$ are a time-dependent probability distribution, and $\mathcal{L}(t)$ is obtained as a time-dependent extension of the fractional Laplacian L^α.

In this work we aim to analyse this generalization based on a variable fractional exponent, potentially able to model better the nonlocal behaviour of the underlying models and discuss some theoretical properties of these models. Moreover, numerical integration methods for these problems are also considered with an eye to more efficient ways to compute the associated matrix-function vector products in view of solving much larger problems.

In the remaining part of the introduction, Section 1.1, we recall some notations related to graphs for a network; then in Section 2 we discuss the definitions of the fractional Laplacian matrix and give some information on the transformed k-path Laplacian. Then, in Section 3, we introduce our generalization to get the non-autonomous extension in (4) and discuss some of its properties. Section 4 briefly introduces the problem of the numerical integration of the underlying non-autonomous systems and the theoretical analysis is completed with some numerical tests on real-world complex networks. Section 5 summarizes the obtained result, and highlights some future research directions.

1.1. Notation and graphs for a network

A well known efficient and clear way to represent the complex interactions of a network is through the use of *graph* models. A *graph* G is defined by a set of *nodes* (or *vertices* $V = \{v_1, \ldots, v_n\}$ and a set of *edges* E that are a subset of the Cartesian product $E \subseteq V \times V$. We set $G = (V, E)$. Cartesian products are ordered, thus if G is an *undirected graph*, we assume that whenever $(v_l, v_j) \in E$ then $(v_j, v_l) \in E$, otherwise G it is a *directed graph*. To avoid repeating this specification, we denote as $\{v_l, v_j\}$ the unordered pairs.

A weighted (undirected) graph $G = (V, E, W)$ is then obtained by considering a (symmetric) weight matrix W with nonnegative entries $(W)_{i,j} = w_{i,j} \geq 0$ and such that $w_{i,j} > 0$ if and only if (v_i, v_j) is an edge of G. If all the nonzero weights have value 1 we omit the weight specification.

We call a *walk* in G a sequence of edges which joins a sequence of vertices in V. if all vertices (and thus all edges) in the walk are distinct we call it a *path*. In case of a direct graph, all the edges in a path should point in the same direction. An undirect graph is *connected* if for each distinct pairs of nodes there is a walk between them. A directed graph is *strongly connected* if for each distinct pairs of nodes v_i, v_j, there is a direct walk from v_i to v_j. The (geodesic) *distance* $d(u, v)$ between two vertices $u, v \in V$ is defined as the length of the shortest path connecting them, where the length of a path is intended as the number of edges crossed. Observe that, in the direct case, $d(u, v)$ can be different from $d(v, u)$. Therefore, in that case, d is only a pseudo distance. We call the *diameter* of the graph G with respect

to the geodesic distance d the quantity $d_{\max} = \max_{u,v \in V} d(u,v)$, i.e. the length of the longest shortest path.

For a direct and an undirect graph G, we introduce the *adjacency matrix* A as the $n \times n$ matrix with entries

$$(A)_{i,j} = a_{i,j} = \begin{cases} 1, & \text{if } (v_i, v_j) \in E, \\ 0, & \text{otherwise.} \end{cases}$$

The adjacency matrix A of an undirected graph G is always symmetric. In particular, if $G = (V, E)$ is a graph, given two nodes $u, v \in V$, we say that u is adjacent to v and write $u \sim v$, if $(u, v) \in E$. The above relation is symmetric if G is an undirected graph, while in general it is not for a directed graph. Note that for an unweighted graph we have $W = A$.

We introduce also the *incidence matrix* of an undirected graph as the $|V| \times |E|$ matrix B, defined by $B_{ij} = 1$ if the vertex v_i and edge e_j are incident and 0 otherwise. For the incidence matrix of a directed graph an arbitrary sign convention has to be imposed. We assume here that $B_{ij} = -1$ if the edge e_j leaves vertex v_i, 1 if it enters vertex v_i and 0 otherwise. In the weighted case we substitute to the value ± 1 the weight of the associated edge.

For every node $v \in V$, we introduce also the *degree* $\deg(v)$ of v as the number of edges leaving *or* entering v taking into account their weights

$$d_i = \deg(v_i) = \sum_{j\,:\,(v_i,v_j)\in E} w_{i,j}.$$

The degree matrix D is then the diagonal matrix whose entries are given by the degrees of the nodes, i.e.

$$D = \operatorname{diag}(\deg(v_1), \ldots, \deg(v_n)) = \operatorname{diag}(d_1, \ldots, d_n).$$

For directed graphs, it is useful to differentiate the degree of a node v_i respectively to the incoming and outgoing edges. For this reason we consider *in–degrees* and *out–degrees*

$$d_i^{(\text{in})} = \deg_{\text{in}}(v_i) = \sum_{j\,:\,(v_j,v_i)\in E} w_{j,i}, \quad d_i^{(\text{out})} = \deg_{\text{out}}(v_i) = \sum_{j\,:\,(v_i,v_j)\in E} w_{i,j},$$

together with the related diagonal matrices

$$D_{\text{in}} = \operatorname{diag}(\deg_{\text{in}}(v_1), \ldots, \deg_{\text{in}}(v_n)) = \operatorname{diag}(d_1^{(\text{in})}, \ldots, d_n^{(\text{in})}),$$
$$D_{\text{out}} = \operatorname{diag}(\deg_{\text{out}}(v_1), \ldots, \deg_{\text{out}}(v_n)) = \operatorname{diag}(d_1^{(\text{out})}, \ldots, d_n^{(\text{out})}).$$

With this notation, we recall some definitions pertaining to the Laplacian matrix as given in [6].

Let $G = (V, E, W)$ be a weighted undirected graph with weight matrix W, weighted degree matrix D and weighted incidence matrix B. Then the *graph Laplacian* L of G is given by

$$L = D - W = BB^T.$$

The *normalized random walk* version of the graph Laplacian is

$$D^{-1}L = I - D^{-1}W = D^{-1}BB^T,$$

where I is the identity matrix. Observe that $D^{-1}W$ is a row-stochastic matrix, i.e. it is nonnegative with row sums equal to 1. The *normalized symmetric* version is

$$D^{-\frac{1}{2}}LD^{-\frac{1}{2}} = I - D^{-\frac{1}{2}}WD^{-\frac{1}{2}}.$$

If G is unweighted then $W = A$ in the above definitions. As in [6], we assume that every vertex has nonzero degree or that every vertex is not *isolated*.

Let $G = (V, E, W)$ be a weighted directed graph, with degree matrices D_{out} and D_{in}. The nonnormalized directed graph Laplacians L_{out} and L_{in} of G are

$$L_{\text{out}} = D_{\text{out}} - W, \quad L_{\text{in}} = D_{\text{in}} - W. \tag{5}$$

To define the normalized versions, we need to invert either the D_{in} or the D_{out} matrices, but the absence of isolated vertices is no longer sufficient to ensure this since there could be a node with only outgoing or ingoing edges. A first way to overcome this issue could be imposing that every vertex has at least one outgoing and one incoming edge, which is rather restrictive. Otherwise, we could restrict our attention to the subsets of nodes having an out-degree or in-degree different from zero.

2. Non-local navigation strategies

There exist different approaches to induce a nonlocal probability transition on the graph $G = (V, E)$. Given the Laplacian matrix L in (3), consider its αth power L^α, $\alpha \in (0, 1]$, for a symmetric L, i.e. for an undirected G. This can be expressed by decomposition [33] as

$$L^\alpha = X\Lambda^\alpha X^T, \quad \Lambda = \text{diag}(\lambda_1^\alpha, \dots, \lambda_n^\alpha), \quad 0 = \lambda_1 \le \lambda_2 \le \dots \le \lambda_n, \quad X^T X = I_n. \tag{6}$$

For a directed graph, the definition of $f(L) = L^\alpha$ requires the Jordan canonical form (see [6] for details)

$$Z^{-1}LZ = J = \text{diag}(J_1, \dots, J_p), \quad J_k = J_k(\lambda_k) = \begin{bmatrix} \lambda_k & 1 & & \\ & \lambda_k & \ddots & \\ & & \ddots & 1 \\ & & & \lambda_k \end{bmatrix} \in \mathbb{C}^{m_k \times m_k},$$

where Z is nonsingular and $m_1 + m_2 + \dots + m_p = n$, and

$$f(L) = Zf(J)Z^{-1} = Z\,\text{diag}(f(J_1), \dots, f(J_p))Z^{-1}, \tag{7}$$

$$f(J_k) = \begin{bmatrix} f(\lambda_k) & f^{(1)}(\lambda_k) & \dots & \dfrac{f^{(m_k-1)}(\lambda_k)}{(m_k-1)!} \\ & f(\lambda_k) & \ddots & \vdots \\ & & \ddots & f^{(1)}(\lambda_k) \\ & & & f(\lambda_k) \end{bmatrix}, \tag{8}$$

that needs the function $f(z) = z^\alpha$ to be defined on the spectrum of L, i.e. the values

$$f^{(j)}(\lambda_i), \quad j = 0, 1, \dots, n_i - 1, \quad i = 1, \dots s,$$

should exist, where $f^{(j)}$ denotes the jth derivative of f, with $f^{(0)} = f$; we refer back to [6] for the details and to [25] for the theory of matrix functions. In both the directed and undirected case we have that $L^\alpha \mathbf{1} = 0$.

Remark 2.1 (k-path Laplacian): Another approach for inferring nonlocal transitions on a network is represented by the *transformed* k-path *Laplacian*. The k-path Laplacian matrix L_k [17,19] of a connected undirected graph $G = (V, E)$ is related to the k-hopping walks and k-path degree.

k-hopping walk: A k-hopping walk of length l is any sequence of (not necessarily different) nodes $v_1, \dots, v_l, v_{l+1}$ such that $d(v_j, v_{j+1}) = k$ for each $j = 1, 2, \dots, l$;

k-path degree: The k-path degree $\delta_k(v_l)$ of a node v_l is the number of irreducible shortest-paths of length k having v_l as an endpoint.

The k-path analogous of the combinatorial Laplacian in (3) is defined as the square symmetric matrix L_k

$$(L_k)_{l,j} = \begin{cases} -1, & d(v_l, v_j) = k, \\ \delta_k(v_l), & v_l \equiv v_j, \\ 0, & \text{otherwise.} \end{cases}$$

To produce the generalized k-path Laplacian inducing the nonlocal transition probability, we consider the series

$$L_G = L_1 + \sum_{k\geq 2} \frac{1}{k^\alpha} L_k = L + \sum_{k\geq 2} \frac{1}{k^\alpha} L_k, \quad \alpha \geq 0,$$

that is indeed a finite sum since L_k coincides with the zero matrix for each $k > d_{\max}$. Observe that again $L_k \mathbf{1} = 0 \; \forall k \geq 1$, and thus $L_G \mathbf{1} = 0$. For the remaining part of the manuscript, we will focus on the properties of the underlying fractional extension. We refer to [18] for some comparison of the two approaches, and to [14] for a discussion on using different type of series and distances on the graph G.

When we substitute L^α into the heat Equation (1) or into the Schrödinger equation, the solution at time t can be expressed in terms of the matrix exponential as

$$\mathbf{p}(t) = \mathbf{p}_0 \exp(-tL^\alpha),$$
$$\boldsymbol{\psi}(t) = \boldsymbol{\psi}_0 \exp(-t\, i\, L^\alpha),$$

that produce a probability distribution $\mathbf{p}(t)$ and a probability density $|\boldsymbol{\psi}(t)|^2$, respectively, because

$$\mathbf{p}(t)\mathbf{1} = \mathbf{p}_0 \exp(-tL^\alpha)\mathbf{1} = \mathbf{p}_0 \left(I - tL^\alpha + \mathbf{p}_0 \frac{t^2 L^{2\alpha}}{2} - \frac{t^3 L^{3\alpha}}{6} + \dots \right) \mathbf{1} = \mathbf{p}_0 \mathbf{1} = 1,$$

having used $L^\alpha \mathbf{1} = \mathbf{0}$, and analogously for the corresponding Schrödinger system. The second noteworthy property of this characterization of the solution is that for the heat equation we can easily compute the steady state for $t \to +\infty$ for a given α on a graph G.

Let us recall some useful definitions of stability from [23]. The vector field f below is assumed smooth enough to ensure existence, uniqueness, and continuous dependence on the parameters but, in our setting, this will concern only $\alpha(t)$ because f is a linear function of $L^{\alpha(t)}$ and L is constant.

Definition 2.1 (Stability): Let us consider the differential equation

$$\mathbf{x}'(t) = f(t, \mathbf{x}), \quad f : \mathbb{C}^{n+1} \to \mathbb{C}^n, \tag{9}$$
$$f(t, 0) = 0, \quad t \geq 0. \tag{10}$$

- The solution $\mathbf{x} = 0$ is called *stable* if for any $\varepsilon > 0$ and any $t_0 \geq 0$, there is $\delta = \delta(\varepsilon, t_0) > 0$ such that $\|\mathbf{x}_0\| < \delta$ implies $\|\mathbf{x}(t, t_0, \mathbf{x}_0)\| < \varepsilon$ for $t \geq 0$.
- The solution $\mathbf{x} = 0$ is called *uniformly stable* if it stable and δ can be chosen independent of $t_0 \geq 0$.
- The solution $\mathbf{x} = 0$ is called *asymptotically uniformly stable* if it uniformly stable, there exists a $b > 0$ that for every $\eta > 0$ there exists a $T(\eta) > 0$ such that $\|\mathbf{x}_0\| < b$ implies $\|\mathbf{x}(t, t_0, \mathbf{x}_0)\| < \eta$ if $t \geq t_0 + T(\eta)$.

The stability of any nonzero solution of the underlying differential equation is easily derived from the ones above. See, e.g. [23] for other details.

When we deal with the heat equation in (1), and, in general, with any constant coefficients case, stability depends only on the eigenvalues of the Jacobian matrix, i.e. L^α in the case of fractional diffusion. Since L^α is an M-matrix (see [6]) for any value of $\alpha \in (0,1)$, every eigenvalue of $-L^\alpha$ have a nonpositive real part and those with zero real part have a Jordan block of size one, i.e. they are semisimple. Thus, the dynamic is automatically uniformly stable. Moreover, for a connected graph G, we find

$$\mathbf{p}(t) = \mathbf{y}_0 \exp(-tL^\alpha) \to \mathbf{1}^T/n, \quad \alpha \in (0,1).$$

Example 2.2: Consider a simple cycle graph G with $n = 4$ nodes, i.e, $V = 1,2,3,4$, $E = \{\{1,2\},\{2,3\},\{3,4\},\{4,1\}\}$, see Figure 1 on the left. The fractional Laplacian matrix for G can be computed in closed form as

$$L^\alpha = \begin{bmatrix} 2^{\alpha-2}(2^\alpha+2) & -4^{\alpha-1} & 2^{\alpha-2}(2^\alpha-2) & -4^{\alpha-1} \\ -4^{\alpha-1} & 2^{\alpha-2}(2^\alpha+2) & -4^{\alpha-1} & 2^{\alpha-2}(2^\alpha-2) \\ 2^{\alpha-2}(2^\alpha-2) & -4^{\alpha-1} & 2^{\alpha-2}(2^\alpha+2) & -4^{\alpha-1} \\ -4^{\alpha-1} & 2^{\alpha-2}(2^\alpha-2) & -4^{\alpha-1} & 2^{\alpha-2}(2^\alpha+2) \end{bmatrix},$$

while the k-path generalized Laplacian matrix reads as

$$L_G = \begin{bmatrix} 2^{-\alpha}+2 & -1 & -2^{-\alpha} & -1 \\ -1 & 2^{-\alpha}+2 & -1 & -2^{-\alpha} \\ -2^{-\alpha} & -1 & 2^{-\alpha}+2 & -1 \\ -1 & -2^{-\alpha} & -1 & 2^{-\alpha}+2 \end{bmatrix}.$$

These above are indeed essentially different. Indeed, $L^\alpha \xrightarrow{\alpha\to 1} L$ and $L_G \xrightarrow{\alpha\to+\infty} L$, while for $\alpha \to 0$, L_G converges to the Laplacian matrix of the complete graph, and L^α to 1/4 of it; see Figure 1. Moreover, for $t \to +\infty$ we can look at the asymptotic behaviour for a given α in Figure 2, i.e. the stability properties of the solution for both the fractional Laplacian L^α and the generalized k-path Laplacian. Independently from the value of α, we observe that all the components of the probability vector reach the stationary solution given by the uniformly distributed probability on the nodes.

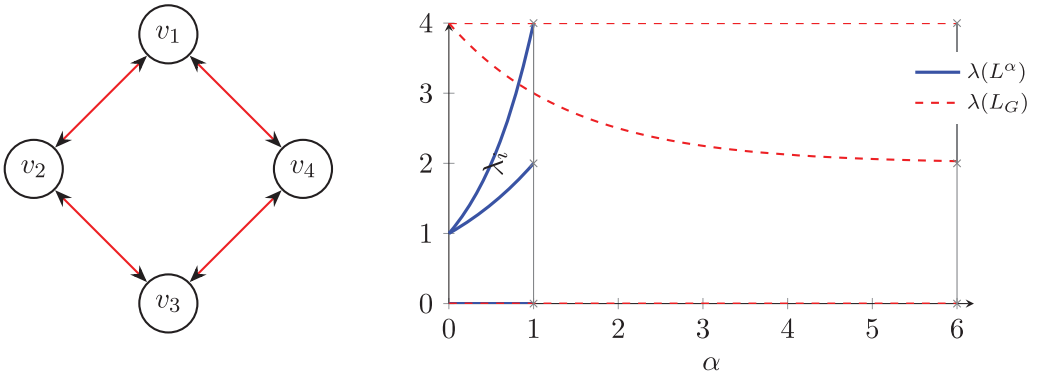

Figure 1. Comparison of the eigenvalues for different values of α between the fractional Laplacian L^α and the generalized k-path Laplacian L_G matrices for the cycle graph on the left. The —— line represents the eigenvalues of the L^α for $\alpha \in [0,1]$, while the - - - represents the Eigenvalues for the generalized k-path Laplacian for $\alpha \in [0,6]$. The $\times$ represents the eigenvalues of the combinatorial Laplacian matrix L.

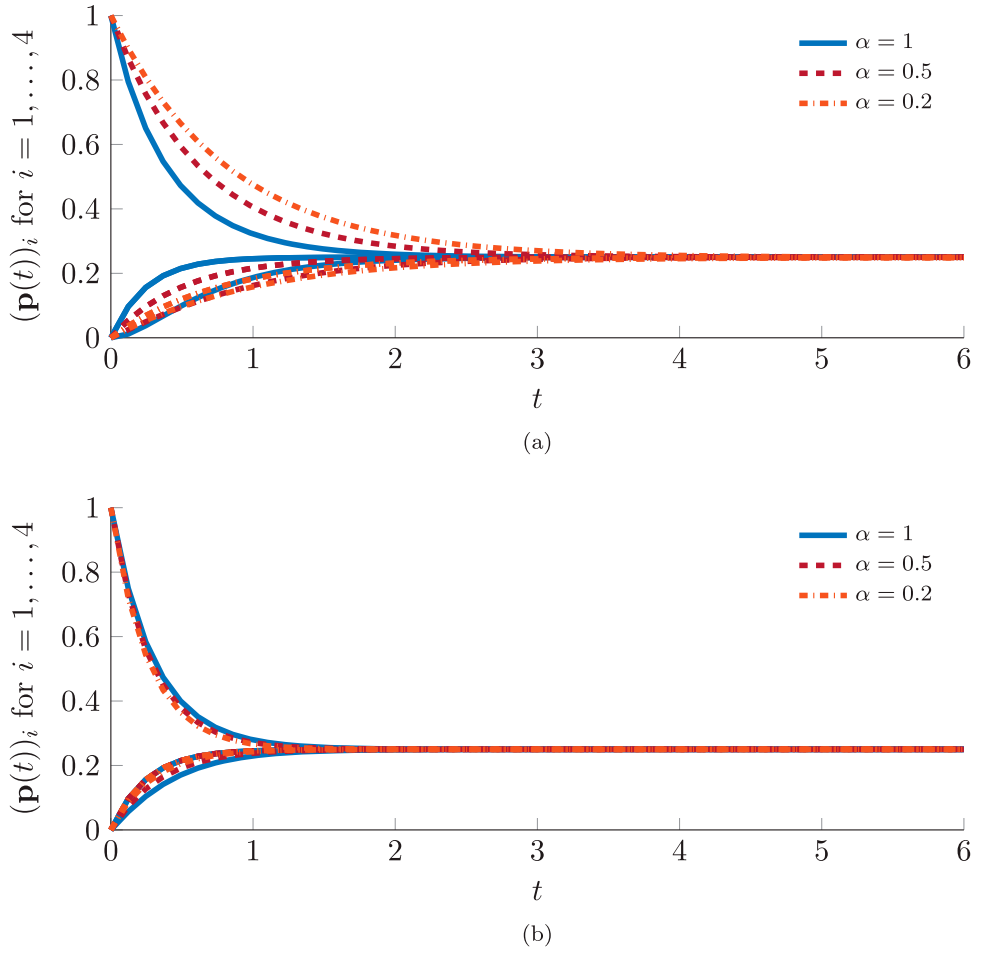

Figure 2. Comparison of the decay behaviour towards the stationary solution using the fractional Laplacian L^α and the generalized k-path Laplacian. (a) With fractional Laplacian matrix L^α (b) With generalized k-path fractional Laplacian matrix.

Remark 2.2: As discussed in [11], we can interpret the fractional navigation strategy as a random walk on a new *complete* graph G' that is built on the same nodes of the original graph. Indeed, the underlying extension is in general not compatible with the dynamics characterizing the original graph model G. If one restricts the random walks on G' to move on the edges of G, these are not *stochastically equivalent* to the random walks on G. In other words, the incompatibility of G' with G means that the graph $\hat{G}$ induced by the normalization $D^{-1}L$ can not be embedded into the normalized graph $\hat{G}'$ related to $D_\alpha^{-1}L^\alpha$, for $D_\alpha = \text{diag}(L^\alpha)$; refer to the analysis in [11] for the details. For our goals here, this is not an issue.

3. Non-local and non-stationary navigation strategies

We can now modify (4) by defining the operator

$$\mathcal{L}(\alpha(t); t) = L^{\alpha(t)}, \quad \alpha : \mathbb{R}_+ \to (0, 1],$$

where we use the function $\alpha(t)$ to modulate the 'quantity of nonlocality' at time t for the probability measures $\mathbf{p}(t)$ and $|\boldsymbol{\psi}(t)|^2$ over G. Such approach is built by extending the fractional Laplacian matrix to a variable order, see, e.g. [22,36,40]. Even if this seems a minor change, two main difficulties

are encountered when moving to the non-autonomous setting. In general, for a system of ordinary differential equations of the form

$$\begin{cases} \mathbf{y}'(t) = \mathcal{A}(t)\mathbf{y}(t), & t > 0, \\ \mathbf{y}(0) = \mathbf{y}_0, \end{cases} \tag{11}$$

the solution *cannot* be expressed as

$$\mathbf{y}(t) = \exp(\mathfrak{A}(t))\mathbf{y}_0,$$

for $\mathfrak{A}(t)$ a primitive of $\mathcal{A}(t)$, consider, e.g. the following example from [39],

$$\mathcal{A}(t) = \begin{bmatrix} 6\sin(12t) - 9\cos^2(6t) - 1 & \frac{9}{2}\sin(12t) + 6\cos(12t) + 6 \\ \frac{9}{2}\sin(12t) + 6\cos(12t) - 6 & -6\sin(12t) + \frac{9}{2}\cos(12t) - \frac{11}{2} \end{bmatrix},$$

for which the solution for $\mathbf{y}_0 = (5, 0)^T$ is given by

$$\mathbf{y}(t) = \begin{bmatrix} 6\sin(12t) - 9\cos^2(6t) - 1 & \frac{9}{2}\sin(12t) + 6\cos(12t) + 6 \\ \frac{9}{2}\sin(12t) + 6\cos(12t) - 6 & -6\sin(12t) + \frac{9}{2}\cos(12t) - \frac{11}{2} \end{bmatrix},$$

that is indeed different from $\mathbf{y}(t) = \exp(\mathfrak{A}(t))\mathbf{y}_0$. Furthermore, we observe also that even if the eigenvalues of $\mathcal{A}(t)$ are $\lambda_1 = -1, \lambda_2 = -10\ \forall t$, the solution $\mathbf{x}(t)$ diverges for $t \to +\infty$, i.e. all eigenvalues with negative real part are no longer sufficient to induce the stability of the resulting system.

The two following sections investigate which properties of the original systems (1) and (2) can be recovered for the non-autonomous versions using α variable with t.

3.1. Existence and uniqueness for our non-autonomous extensions

Let us analyse first existence and uniqueness of the solution of the problem whose Jacobian matrix is the fractional power of the combinatorial Laplacian

$$\begin{cases} \mathbf{p}'(t) = -\mathbf{p}(t)L^{\alpha(t)}, & t > 0, \\ \mathbf{p}(0) = \mathbf{p}_0, & \sum_{j=1}^{n}(\mathbf{p}_0)_j = 1, \end{cases} \quad \alpha(t) : \mathbb{R}_+ \to (0, 1]. \tag{12}$$

Lemma 3.1: *Let $G = (V, E)$ be a simple graph and $\alpha(t) : \mathbb{R}_+ \to (0, 1]$ a continuous function. Then,*

(1) *$z \mapsto z^{\alpha(t)}$ is defined on the spectrum of the Laplacian matrix L for every t;*
(2) *$\exists\, k > 0$ such that $\|L^{\alpha(t)}\| \leq k$ for $t > 0$;*
(3) *$f(t, \mathbf{p}) = -\mathbf{p}L^{\alpha(t)}$ is Lipschitz continuous with respect to $\mathbf{p}$ for $t > 0$.*

Proof: The first item is just a corollary of [6, Theorem 2.6], since the conditions on the existence of the derivatives are to be considered with respect to the z variable, and $\forall\, t > 0$ we have that $\alpha(t) \in (0, 1]$. For an undirected graph, since the power function is monotonically increasing, we bound $\|L^{\alpha(t)}\|_2 \leq \lambda_n^M = k$ for $M = \max_{t\in\mathbb{R}} \alpha(t)$. For the directed case, and, e.g. the out-degree Laplacian, a more involved form for the constant k can be obtained [6, Section 3.2], and [7, Section 4]. In both cases the obtained k can be used as the Lipschitz constant as below

$$\|\mathbf{x}L^{\alpha(t)} - \mathbf{y}L^{\alpha(t)}\| \leq k\|\mathbf{x} - \mathbf{y}\|.$$

■

Theorem 3.2: *Under the hypothesis of Lemma* 3.1, *there exists a unique solution for the Cauchy problem* (12) *for* $t > 0$.

Proof: The system in (12) is linear homogeneous with $(L^{\alpha(t)})_{i,j} = l_{i,j}(t) \in \mathcal{C}^0$ a matrix of continuous real functions in t. This is indeed a classical case under which existence and uniqueness are guaranteed by, e.g. [15, Theorem 5.1] or any other book covering fundamentals on ordinary differential equations. ■

To build explicitly the solution of (12), a commutativity result is of fundamental importance. Indeed, if the matrix $L^{\alpha(t)}$ commutes with its antiderivative then we can express the solution by using the exponential of the antiderivative of $L^{\alpha(t)}$.

Proposition 3.3: *Given a graph* $G = (V, E)$, *let* L *be its combinatorial Laplacian matrix in* (3) *and* $\alpha : \mathbb{R}^+ \to (0, 1]$ *a continuous function. Then, the matrices* $-L^{\alpha(t)}$ *and* $\exp(-\mathfrak{L}(t)) = \exp(-\int_0^t L^{\alpha(\tau)}\, d\,\tau)$ *commute.*

Proof: For an undirected graph G, L is a symmetric matrix, then we can compute $-L^{\alpha(t)}$ as in (6). Thus,

$$
\begin{aligned}
-L^{\alpha(t)} \exp(-\mathfrak{L}(t)) &= -X\Lambda^{\alpha(t)}X^T \exp\left(-\int_0^t X\Lambda^{\alpha(\tau)}X^T \,\mathrm{d}\tau\right) \\
&= X\left(-\Lambda^{\alpha(t)} \exp\left(-\int_0^t \Lambda^{\alpha(\tau)}\,\mathrm{d}\tau\right)\right)X^T \\
&= X\left(-\exp\left(\int_0^t -\Lambda^{\alpha(\tau)}\,\mathrm{d}\tau\right)\Lambda^{\alpha(t)}\right)X^T \\
&= -X\exp\left(-\int_0^t \Lambda^{\alpha(\tau)}\,\mathrm{d}\tau\right)X^T X\Lambda^{\alpha(t)}X^T \\
&= -\exp(-\mathfrak{L}(t))L^{\alpha(t)}.
\end{aligned}
$$

For a directed graph, we need to consider the definition through the Jordan canonical form in (7)–(8), i.e. we can rewrite $-L^{\alpha(t)}\exp(\mathfrak{L}(t))$ as

$$
\begin{aligned}
-L^{\alpha(t)} \exp(\mathfrak{L}(t)) &= -ZJ^{\alpha(t)}Z^{-1} \exp\left(-\int_0^t ZJ^{\alpha(\tau)}Z^{-1}\,\mathrm{d}\tau\right) \\
&= Z\left(-J^{\alpha(t)} \exp\left(-\int_0^t J^{\alpha(t)}\,\mathrm{d}\tau\right)\right)Z^{-1},
\end{aligned}
$$

by using Lemma 3.1, and observing that $f(t) = \lambda_k^{\alpha(t)}$ is integrable. Now $\exp(J^{\alpha(t)})$ is a matrix exponential of a block-diagonal matrix, thus it is block diagonal itself, and the product of the block-diagonal matrix commutes if and only if the product of the blocks commutes. Therefore, we can reduce the previous computation on a generic Jordan block J_k. By construction, each block is an upper triangular Toeplitz matrix, i.e. is a matrix with constant entries along the diagonals. The conclusion follows from the fact that the product of upper triangular Toeplitz matrices is commutative because it can be expressed as the product of two matrix polynomials for the same matrix; see [12] and [9, Chapter 2]. ■

Theorem 3.4: *Given a graph* $G = (V, E)$, *let* L *be its combinatorial Laplacian matrix in* (3) *and* $\alpha : \mathbb{R}^+ \to (0, 1]$ *a continuous function. Then, the problem in* (12) *admits a solution* $\mathbf{p}(t)$ *on every interval* $[0, T]$ *and* $\|\mathbf{p}(t)\|_1 = 1\ \forall t \in [0, T]$.

Proof: The proof follows from Theorem 3.2 and from the property that the matrix $L^{\alpha(t)}$ commutes with its antiderivative by Proposition 3.3. Indeed, we can express the solution in closed form with the exponential of the antiderivative of $L^{\alpha(t)}$, i.e. the solution of (12) can be expressed as

$$\mathbf{p}(t) = \mathbf{p}_0 \exp\left(-\int_0^t L^{\alpha(\tau)}\,\mathrm{d}\tau\right),$$

whenever

$$L^{\alpha(t)}\int_0^t L^{\alpha(\tau)}\,\mathrm{d}\tau - \int_0^t L^{\alpha(\tau)}\,\mathrm{d}\tau L^{\alpha(t)} = 0,$$

that is exactly what we proved in Proposition 3.3. Then, to prove that

$$\|\mathbf{p}(t)\|_1 = \mathbf{p}(t)\mathbf{1} = 1,$$

we have only to prove that $\mathfrak{L}(t)\mathbf{1} = \mathbf{0}\ \forall t \geq 0$, and indeed

$$\mathfrak{L}(t)\mathbf{1} = \int_0^t L^{\alpha(\tau)}\,\mathrm{d}\tau\mathbf{1} = \int_0^t L^{\alpha(\tau)}\mathbf{1}\,\mathrm{d}\tau = \int_0^t \mathbf{0}\,\mathrm{d}\tau = \mathbf{0}.$$

■

Remark 3.1: The proof of Proposition 3.3, and, therefore, of Theorem 3.4, depends on one hand on the fact that all the matrices involved are diagonalized by the same transform that is independent of t, and, on the other, the Jordan blocks are upper triangular Toeplitz matrices. These properties are inherited from the definition in (7)–(8). Therefore, both the results can be extended to other matrix functions with constant L depending on a variable parameter.

3.2. Stability for our non-autonomous extensions

Let us discuss the stability of (12). The classical definitions of stability and asymptotic stability, due to Lyapunov, can be useful for the study of autonomous differential equations. For our nonautonomous equations, however, the concepts of uniform stability and uniform asymptotic stability are more appropriate; see W. A. Coppel [16, Chapter 1].

A special case is when $\mathcal{L}(t)$ is a T-periodic function for which it is possible to apply Floquet Theorem, see, e.g. [23, Chapter III.7].

Theorem 3.5 (Floquet): *Every fundamental matrix solution $P(T)$ of*

$$P'(t) = -P(t)\mathcal{L}(t), \quad t > 0, \quad \exists\, T > 0 : \mathcal{L}(t+T) = \mathcal{L}(t), \quad \forall\, t > 0, \tag{13}$$

has the form

$$P(t) = X(t)e^{Bt}, \tag{14}$$

where $X(t)$, B are $n \times n$ matrices, $X(t+T) = X(t)$ for all t, and B is a constant.

The stability studied by the *characteristic exponent* λ in (13), i.e. the complex number λ for which $x(t)e^{\lambda t}$ is a nontrivial solution of (13) with $\mathbf{x}(t) = \mathbf{x}(t+T)$, implies that there exists a representation of the solution (14) for which the values of λ are the eigenvalues of B in (14).

Theorem 3.6 ([23, Theorem 7.2]): (1) *A necessary and sufficient condition for the system* (13) *to be uniformly stable is that the characteristic exponents have real parts ≤ 0 and the ones with zero real parts have simple elementary divisors.*

(2) *A necessary and sufficient condition for the system* (13) *to be uniformly asymptotically stable is that all the characteristic exponents have real parts* < 0. *If this is the case and* $P(t)$ *is a matrix solution of* (13), *then there exist* $K > 0$, $\eta > 0$ *such that* $\|P(t)P^{-1}(s)\| \leq K \exp(-\eta(t-s))$, *for* $t \geq s$.

Let us stress that the characteristic exponents are defined only after the solutions of (13) are computed. In general, there is no straightforward relation between the characteristic exponents and the eigenvalues of $\mathcal{L}(t)$.

Fortunately, a much more general result is available. Indeed, we can prove the uniformly asymptotical stability for our linear differential equation also if $\mathcal{L}(t)$ is not T-periodic; see W. A. Coppel [16, Chapter 1], provided that the exponent scalar function $\alpha(t)$ is regular enough.

Theorem 3.7 ([16]): *If there exist* $K > 0$, $\eta > 0$ *such that* $\|P(t)P^{-1}(s)\| \leq K \exp(-\eta(t-s))$, P *fundamental matrix solution of* (12) *for* $t \geq s$, *the IVP* (12) *is uniformly asymptotically stable.*

Theorem 3.8: *Given a (strongly) connected graph* $G = (V, E)$, *let* L *be its combinatorial (out-degree) Laplacian matrix in* (3) *and* $\alpha : \mathbb{R}^+ \to (0, 1]$ *a continuous function. Then, the solution* $\mathbf{p}(t)$ *of problem* (12) *is uniformly asymptotically stable.*

Proof: Let $P(t)$ be the matrix solution of (12), i.e. $P(t) = \exp(-\int_0^t L^{\alpha(\tau)}\, d\tau)$, we will prove that there exists $K > 0$, and $\eta > 0$ such that

$$\|P(t)P^{-1}(s)\| \leq K \exp(-\eta(t-s)), \quad t \geq s, \tag{15}$$

so that we can apply Theorem 3.6. We start from the case in which G is an undirected graph, thus, by using the Euclidean norm, by direct computation, we find

$$\begin{aligned}
\|P(t)P^{-1}(s)\|_2 &= \left\| \exp\left(-\int_0^t L^{\alpha(\tau)}\, \mathrm{d}\tau\right) \exp\left(\int_0^s L^{\alpha(\tau)}\, \mathrm{d}\tau\right) \right\| \\
&= \left\| X \exp\left(-\int_0^t \Lambda^{\alpha(\tau)}\, \mathrm{d}\tau\right) \exp\left(\int_0^s \Lambda^{\alpha(\tau)}\, \mathrm{d}\tau\right) X^T \right\| \\
&= \left\| \exp\left(\int_t^s \Lambda^{\alpha(\tau)}\, \mathrm{d}\tau\right) \right\| \\
&\leq \exp\left(\left\| \int_t^s \Lambda^{\alpha(\tau)}\, \mathrm{d}\tau \right\| \right) \leq \exp\left((s-t) \max_{\tau \in \mathbb{R}} \|\Lambda^{\alpha(\tau)}\| \right) \\
&\leq \exp(-\beta(t-s)),
\end{aligned}$$

from which we find (15) for $K = 1$ and

$$\eta = \beta = \max_{i,\tau} \lambda_i(L)^{\alpha(\tau)},$$

where $\lambda_i(L)$ is the i-th eigenvalue of the Laplacian. For a directed graph, we suppose that the Laplacian is diagonalizable and we get the same result but with

$$K = \|Z\|_2 \|Z^{-1}\|_2 = \mathrm{cond}_2(Z),$$

cond_2 the 2-norm condition number of the matrix Z diagonalizing L.

If L cannot be diagonalized, a similar approach can be adapted by using a Jordan decomposition of the Laplacian matrix. ■

The results on stability analysis we have obtained here could be applied to neural networks, by leveraging, e.g. the results in [32], and the references therein. Other possible applications of these techniques are in [4,13,30,31].

4. Integrating the non-autonomous systems

Let us now consider the numerical integration of (12) to see the evolution of the probability distributions on the graphs.

Here we use the MATLAB's ode packages `ode45` and `ode15s`. Both are methods with local error estimators that can control and adapt the stepsize to reach the prescribed accuracy (here we request a relative tolerance `reltol`$= 10^{-6}$). The first method is a fourth-order nonstiff integrator based on (explicit) Runge-Kutta-Fehlberg formulas while `ode15s` is based on the numerical differentiation formulas (NDFs, a generalization of BDFs; see [27] for details on BFDs) of orders from 1 to 5. The latter is based on implicit schemes and is able to manage *stiff* problems. For more details on formulas for numerical integration of ODEs, in particular of their consistence, convergence and stability, see, e.g. [27]. In particular, for the definitions of stiff problem and stiffness see [27, Chapter 6].

4.1. Operations with L^α

We considered the use of implicit time-step integration to avoid possible severe stepsize restrictions to satisfy stability requirements of the underlying formulas that we experienced in some tests even for not so long final times. Implicit time-step integrators for a problem of the form (11) require the solution of a sequence of linear systems of the form

$$(\alpha_m I + \delta_m \beta_m \mathcal{A}(t_m))\, \mathbf{y}^{(m)} = \delta_m \mathbf{v}^{(m-1)}, \quad m = 0, 1, \ldots, n_t, \tag{16}$$

where δ_m is the m-th time step, the coefficients $\{\alpha_m, \beta_m\}_{m=0}^{\ell}$ are selected depending on the particular formula used, $\mathbf{v}^{(m-1)}$ is a suitable combination of the vectors containing previous time steps and the $\{\alpha_m, \beta_m\}$ coefficients. See, e.g. [1, Section 4.1] for the use of linear multistep formulas in a similar context and [27] for a general discussion.

In the case we are treating here, we use the above mentioned MATLAB time-step integrators package. In principle, they can be invoked by employing only the dynamics of the associated differential problems. This means that we need a routine that can evaluate $\mathbf{v}.\mathcal{A}$ for the $\mathbf{v}$ generated by the underlying integrator to handle

$$f(x) = -x^{\alpha(t)}, \tag{17}$$

or

$$f(x) = -ix^{\alpha(t)}, \tag{18}$$

for computing $\mathbf{v}f(L)$. Then, to formulate and solve the linear system (16), the routine assembles the whole matrix at each new time-step and utilizes a direct solver. The building phase for the sequence of linear systems (16), if no further information are given to the integrator, is completed by performing several matrix-vector products with $L^{\alpha(t)}$. To reduce the computing time, we provide to the integrator a routine to build directly the matrix $L^{\alpha(t)}$ for every t.

A further reduction in the timings could result by implementing a code for computing directly the matrix function-vector product with

$$F(x; t) = \left(\alpha_m + \delta_m \beta_m x^{\alpha(t)}\right)^{-1}, \quad m = 0, 1, \ldots, n_t,$$

for $\delta_m \mathbf{v}^{(m-1)} F(\mathcal{A}; t_m)$. This procedure can be based on the techniques for the computation of matrix function times a vector product with the functions (17), and (18). For symmetric positive definite matrices there exist several efficient approaches, either based on various type of quadrature formulas [2,3,8,24,26], or on Krylov methods [1,28,29]. The case we want to deal with here needs an extra care because of the presence of the zero eigenvalue in L for which we refer to the strategies introduced in [7]. Having selected the procedure for computing the αth power, then the extension to the computation of the $F(x, t)$ could be addressed with the techniques discussed in [1, Section 4.1].

4.2. Numerical examples

We consider numerical examples on some real-world complex networks from [35], and choices for the values of the function $\alpha(t)$ from [22]. All the experiments run on MATLAB 9.6.0.1072779 (R2019a) installed on a Linux machine with an Intel^R Core^{TM} i7-8750H CPU @ 2.20 GHz processor, and 16 Gb of RAM.

Example 4.1: We consider as the first example of this section the *Zachary's Karate club network* [5,35]. This is a small (undirected) social network of a university karate club with $n = 34$ nodes. We simulate both the dynamics from (4) for some choice of $\alpha(t)$ from [22]. We start the simulation from a random vector sampled from a uniform distribution across the nodes of the network.

In Figure 3 we observe that the use of the different $\alpha(t)$ alters the evolution of the probability. Specifically, for each time step, we report the value of the probability at the given node. In every case, after a long time, all the solutions reach the steady-state, represented by the uniform color, and we observe different transient behaviour.

We also observe how this behaviour is maintained even in the case of *only continuous* $\alpha(t)$ functions. To this end, we consider the periodic sawtooth function in Figure 4(a) alternating between the values (0.05, 0.75].

In this case, the evolution of the probability distribution behaves again as intended. If we look at the evolution for a given node in Figure 4(b), we observe that the probability 'oscillates' between the behaviour given by the two fixed value of $\alpha(t)$, the two extremes of the sawtooth function.

A more complex behaviour is highlighted by Schrödinger model, see Figure 5, in which we do not reach a steady-state, as in the case of a fixed $\alpha \in (0, 1]$. For all tests, we have a different behaviour in the intermediate times, showing the effect of the new exploration strategy.

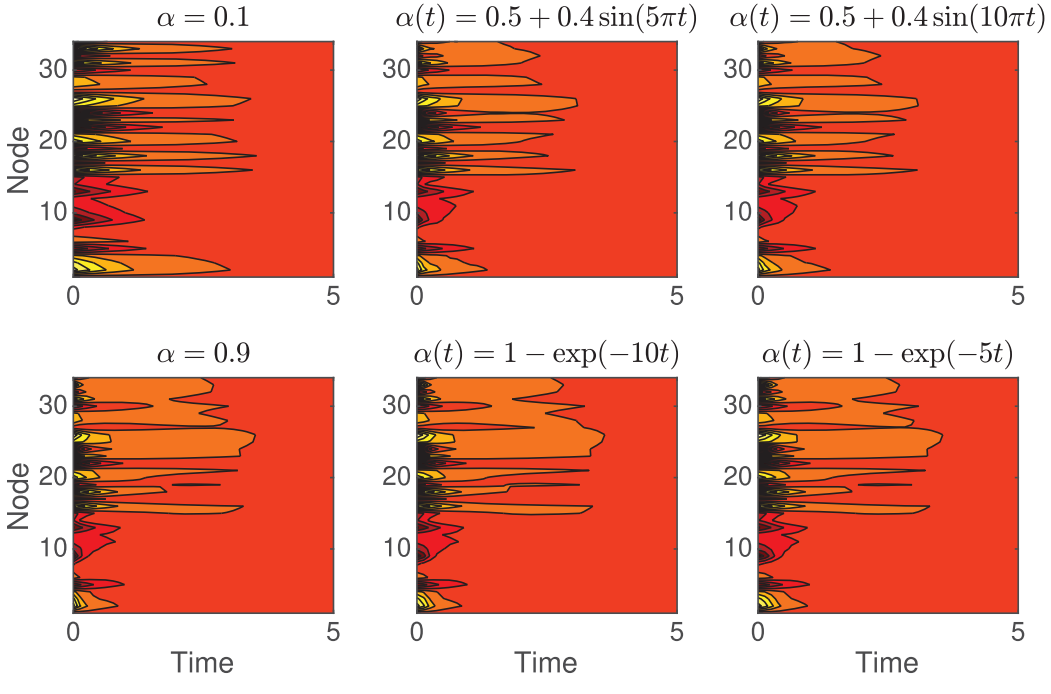

Figure 3. Zachary's karate club network [5,35]. This is a small social network of a university karate club with $n = 34$ nodes. Evolution of the probability $\mathbf{p}_i(t)$ for $i = 1, \ldots, 34$, $t \in [0, 10]$ for different choices of $\alpha(t)$ and the Heat equation dynamics from (4).

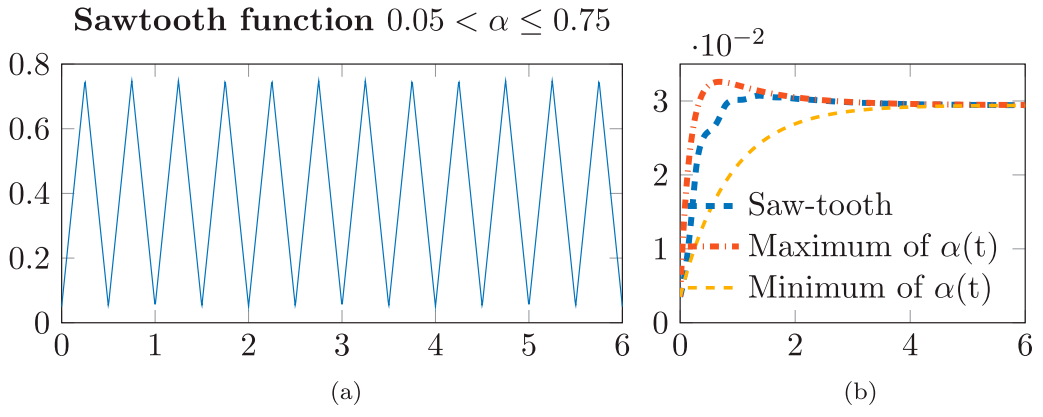

Figure 4. Zachary's Karate club network [5,35]. Example of the trajectories obtained by employing a function $\alpha(t)$ that is only continuous. Comparison with the trajectories obtained with the constant fractional Laplacian with values the maximum and minimum of the $\alpha(t)$ function. (a) Sawtooth $\alpha(t)$ function (b) Probability evolution for a selected node.

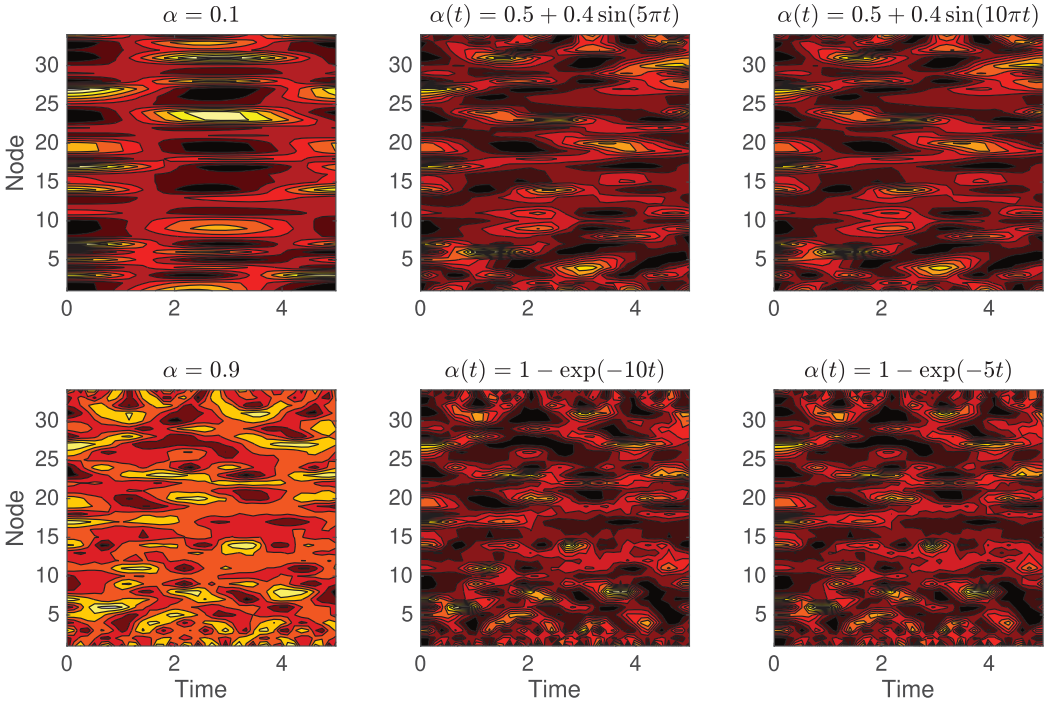

Figure 5. Zachary's Karate club, Schrödinger model [5,35]. A small social network of a university Karate club with $n = 34$ nodes.

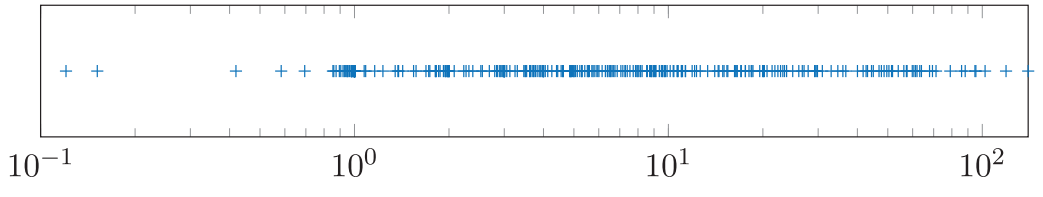

Figure 6. Eigenvalue distribution of the Laplacian matrix of the graph of US Airlines in 1997. Source of the graph data: [35].

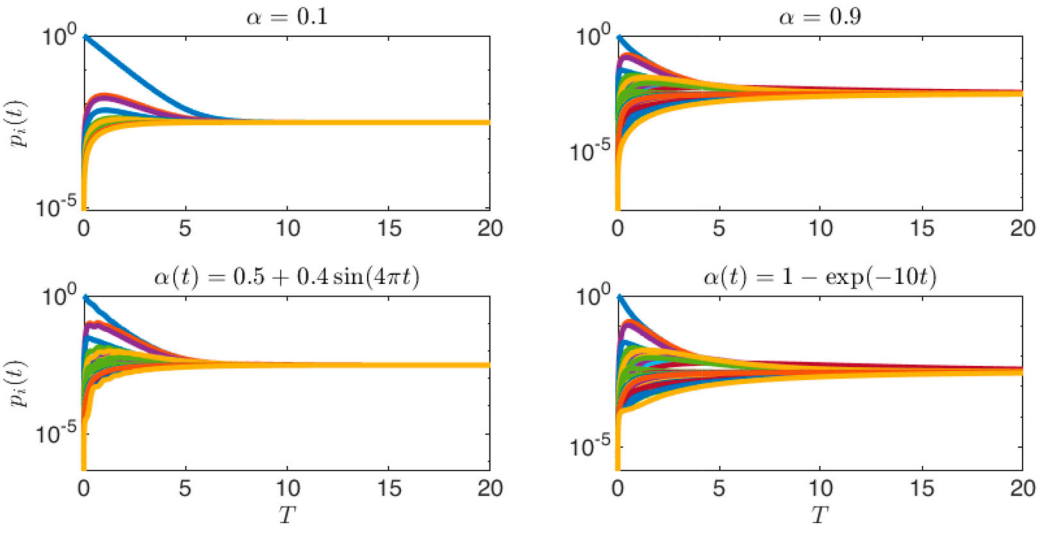

Figure 7. Comparison of short-term results of US Airlines in 1997 integrated using ode15s. Source of the graph data: [35].

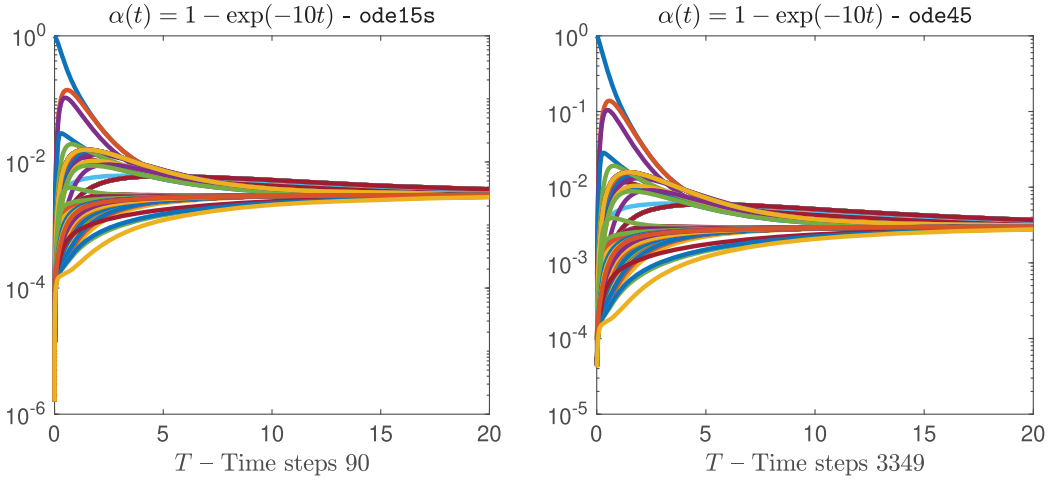

Figure 8. Comparison of short-term results of US Airlines in 1997 integrated using `ode45` and `ode15s` $\alpha(t) = 1 - \exp(-10t)$. Transition probabilities are depicted in logarithmic scale to better highlight the differences between the transitions. Source of the graph data: [35].

Example 4.2: To look more closely at the convergence towards the steady-state, we consider a larger graph based on US airlines in 1997, where the graph is undirected with 332 nodes. The (real and nonnegative) eigenvalue distribution of the underlying Laplacian matrix is depicted in Figure 6.

In the Figures 7, 8 and 9 we report the output and, in particular, the evolution of the probability distribution for runs with short final times. This shows some interesting performances of the functions $\alpha(t)$ considered. Moreover, the Figures 8 and 9 are useful to observe a moderate stiffness phenomena that can be present even in small graphs, and that is clearly highlighted by the difference in the number of time steps generated by the underlying stiff and nonstiff time-step integrators. In particular, for $\alpha(t) = 1 - \exp(-10t)$ in Figure 8 we have that `ode45` employs 3349 time steps, while `ode15s` needs just 90. As expected, the difference is less pronounced in Figure 9, where the periodic transition

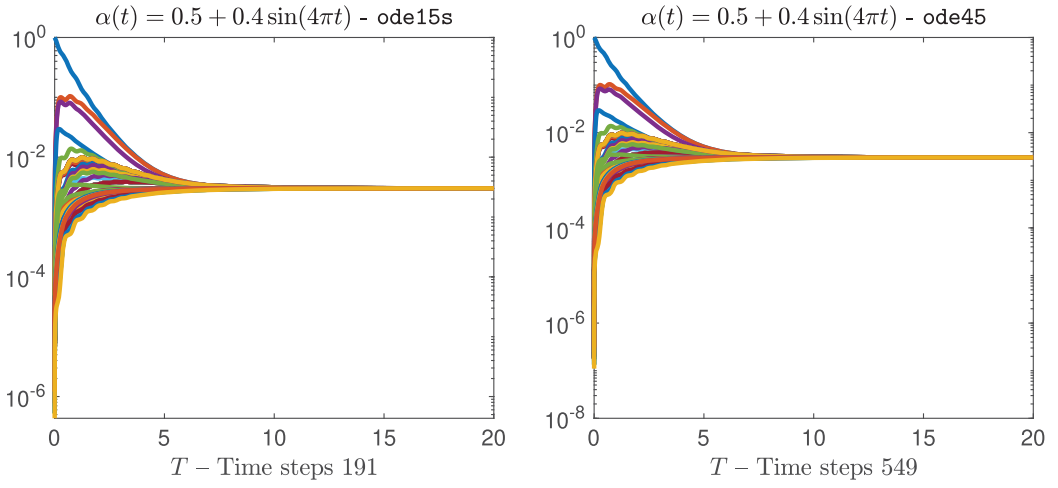

Figure 9. Comparison of short-term results of US Airlines in 1997 integrated using `ode45` and `ode15s`, $\alpha(t) = 0.5 + 0.4\sin(4\pi t)$. Source of the graph data: [35].

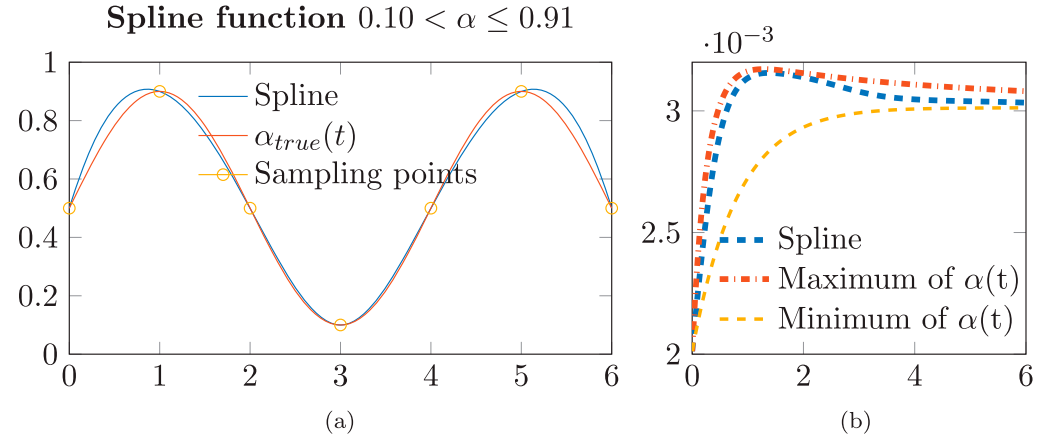

Figure 10. US Airlines in 1997 [35]. Example of the trajectories obtained by employing a function $\alpha(t)$ with reduced regularity. Comparison with the trajectories obtained with the constant fractional Laplacian matrix with values the maximum and minimum of the $\alpha(t)$ function. (a) Spline approximation of the $\alpha_{\text{true}}(t)$ function. (b) Probability evolution for a selected node.

$\alpha(t) = 0.5 + 0.4\sin(4\pi t)$ has been adopted instead: `ode45` employs 549 time steps while `ode15s` employs 191.

To conclude the example, consider using a less regular $\alpha(t)$. Specifically, we use a sampling of the function $\alpha_{\text{true}}(t) = 0.5 + 0.4\sin(\pi t/2)$ at points $t_k = k, k = 0, 1, \ldots, 6$. Then, for integrating the system, we use the piecewise polynomial form of the cubic spline interpolating $\alpha(t)$ on these data; see Figure 10(a). From Figure 10(b), that represents the probability evolution for an arbitrary node of the network, we observe again the same behaviour shown in the other cases, i.e. the probability evolves mimicking the extreme cases, at least in part.

Example 4.3: Let us now consider a *directed* network. We simulate the evolution of the probability distributions on the weighted `cage8` graph from the van Heukelum collection [38]. The weights on the adjacency matrix describe the transition probabilities between equivalence classes of the configurations, for an applied field of $E = (0.1, 0.1, 0.1)$ and a polymers of 8 monomers in a cage model of DNA electrophoresis. We model the evolution of the probability $\mathbf{p}(t)$ for $t \in [0, 5]$ for the choices of

$\alpha(t)$ from Figure 3, and the heat equation dynamics from (4). That is, we look at the transition function $\alpha(t)$ given by the two fixed values, the two oscillating functions and the exponential transitions. Since the network is now directed, we need to choose which Laplacian matrix we adopt. For this case we consider the out-degrees, i.e. L_{out} in (5).

To depict a clearer picture, we report in Figure 11 the evolution of the probability of a single node. We can observe rapid oscillations in the transient phase, while the oscillations settle to the steady state more slowly.

Example 4.4: The last test case we consider is the *EU-Road network* [37]. This is the international E-road network for roads that are mostly located in Europe. The network is undirected, with nodes representing cities and links denoting e-road between two cities, and is neither *scale-free* nor *small-world*. Moreover, since the graph has more than one connected components, we restrict the analysis to the largest component of the network consisting of 1039 nodes and 1355 edges.

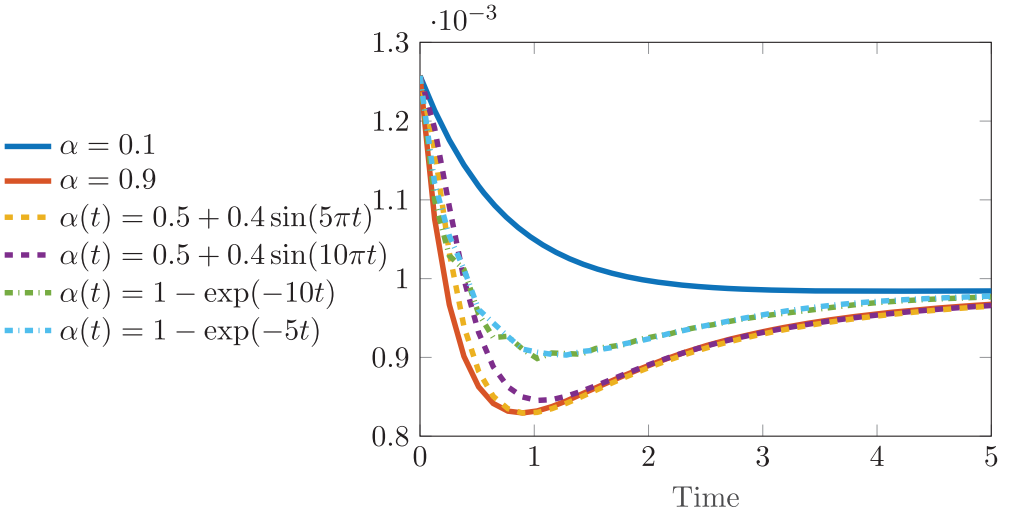

Figure 11. `Cage8` network [38]. This is a cage model of DNA electrophoresis with $n = 1015$ nodes. Evolution of the probability $\mathbf{p}_i(t)$ for $i = 6$, $t \in [0, 5]$ for different choices of $\alpha(t)$ and the Heat equation dynamics from (4).

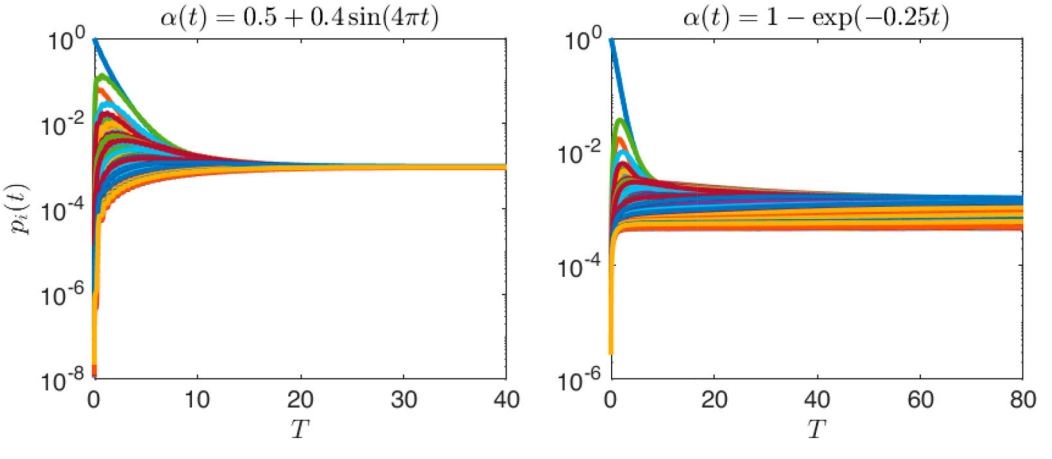

Figure 12. Euroad network. Source of the graph data: [35,37].

In the figures in 12, we report the output and, in particular, the evolution of the probability distribution for two different runtimes and $\alpha(t)$. We can observe that the oscillations reach the steady-state faster than the one in which our 'attention span' rapidly reaches the value 1. Indeed, if we go 'one road at a time' across the whole of Europe, we need potentially much more time to explore every place.

5. Conclusions

We extended the nonlocal exploration of complex networks utilizing a time-varying function $\alpha = \alpha(t)$ for the fractional Laplacian matrix used as the Jacobian of an initial value problem for the evolution of the underlying probability distributions (see [6,33,34]). In particular, we proved existence, uniqueness, and asymptotic stability properties of the solution of a model based on the heat equation. Interesting (moderate) stiffness phenomena of the underlying system of differential equations on some real-world complex networks are also observed in some numerical experiments involving simulations of the evolution of the probability distributions for complex networks.

There are some directions in which we plan to extend this study. The first is the generalization to the non-autonomous version of the transformed k-path Laplacian briefly discussed in Remark 2.1, even if the formulation of this case can be achieved straightforwardly by modifying the k-path operator to

$$\mathcal{L}_G(\alpha(t);t) = L_1 + \sum_{k\geq 2} \frac{1}{k^{\alpha(t)}} L_k, \quad \alpha : \mathbb{R}_+ \to \mathbb{R}_+.$$

This extension does not falls under the observation in Remark 3.1, since the matrices $\mathcal{L}_G(\alpha(t);t)$, even in the symmetric case, cannot be diagonalized by the same transformation in general.

The second is to (i) extend the approach in [1] by working with a variable order integrator and the singular M-matrix L, by applying some of the techniques proposed in [7] and (ii) use computationally efficient techniques to solve (16) generalizing those proposed in [10].

Acknowledgments

We would like to thank the referees for their appreciation and constructive comments. In particular, the papers [4,13,30–32] have been suggested by one of the referees.

Disclosure statement

No potential conflict of interest was reported by the author(s).

Funding

The authors are partially supported by INDAM-GNCS and by the INdAM-GNCS project 'Metodi numerici per l'analisi di modelli innovativi di reti complesse' CUP E55F22000270001. D. Bertaccini acknowledges the MIUR Excellence Department Project awarded to the Department of Mathematics, University of Rome Tor Vergata, CUP E83C18000100006 and the Tor Vergata University 'Beyond Borders' program through the project ASTRID, CUP E84I19002250005.

References

[1] L. Aceto, D. Bertaccini, F. Durastante, and P. Novati, *Rational Krylov methods for functions of matrices with applications to fractional partial differential equations*, J. Comput. Phys. 396 (2019), pp. 470–482. Available at https://doi.org/10.1016/j.jcp.2019.07.009. MR 3989621.

[2] L. Aceto and P. Novati, *Rational approximation to the fractional Laplacian operator in reaction–diffusion problems*, SIAM J. Sci. Comput. 39 (2017), pp. A214–A228. Available at https://doi.org/10.1137/16M1064714. MR 3597163.

[3] L. Aceto and P. Novati, *Rational approximations to fractional powers of self-adjoint positive operators*, Numer. Math. 143 (2019), pp. 1–16. Available at https://doi.org/10.1007/s00211-019-01048-4. MR 3987166.

[4] P. Agarwal, M.R. Sidi Ammi, and J. Asad, *Existence and uniqueness results on time scales for fractional nonlocal thermistor problem in the conformable sense*, Adv. Differ. Equations 2021 (2021), p. 162. Available at https://doi.org/10.1186/s13662-021-03319-7.

[5] N. Beerenwinkel, B. Schmidt, H. Walter, R. Kaiser, T. Lengauer, D. Hoffmann, K. Korn, and J. Selbig, *Diversity and complexity of hiv-1 drug resistance: A bioinformatics approach to predicting phenotype from genotype*, Proc. Natl. Acad. Sci. 99 (2002), pp. 8271–8276. Available at https://www.pnas.org/content/99/12/8271.
[6] M. Benzi, D. Bertaccini, F. Durastante, and I. Simunec, *Non-local network dynamics via fractional graph laplacians*, J. Complex Netw. 8 (2020), p. cnaa017. Available at https://doi.org/10.1093/comnet/cnaa017. MR 4130854.
[7] M. Benzi and I. Simunec, *Rational Krylov methods for fractional diffusion problems on graphs*, BIT Numer. Math. 62 (2021), pp. 357–385. Available at https://doi.org/10.1007/s10543-021-00881-0.
[8] D. Bertaccini and F. Durastante, *Computing functions of very large matrices with small TT/QTT ranks by quadrature formulas*, J. Comput. Appl. Math. 370 (2020), p. 112663. Available at https://doi.org/10.1016/j.cam.2019.112663. MR 4046619.
[9] D. Bertaccini, P. Zellini, and C. Di Fiore, *Complessità e iterazione numerica. Percorsi, matrici e algoritmi veloci nel calcolo numerico*, Programma di mat. fisica elettronica, Bollati Boringhieri, 2013.
[10] D. Bertaccini and F. Durastante, *Computing function of large matrices by a preconditioned rational Krylov method*, in *Numerical Mathematics and Advanced Applications – ENUMATH 2019*, Lect. Notes Comput. Sci. Eng. Vol. 139, Springer, Cham, 2021, pp. 343–351. Available at https://doi.org/10.1007/978-3-030-55874-1_33. MR 4266513.
[11] D. Bianchi, M. Donatelli, F. Durastante, and M. Mazza, *Compatibility, embedding and regularization of non-local random walks on graphs*, J. Math. Anal. Appl. 511 (2022), p. 126020. Available at https://doi.org/10.1016/j.jmaa.2022.126020. MR 4379318.
[12] D. Bini and V.Y. Pan, *Polynomial and Matrix Computations: Fundamental Algorithms. Vol. 1*, Progress in Theoretical Computer Science, Birkhäuser Boston, Inc., Boston, MA, 1994, Available at https://doi.org/10.1007/978-1-4612-0265-3, MR 1289412.
[13] N. Boonsatit, G. Rajchakit, R. Sriraman, C.P. Lim, and P. Agarwal, *Finite-/fixed-time synchronization of delayed Clifford-valued recurrent neural networks*, Adv. Differ. Equations 2021 (2021), p. 276. Available at https://doi.org/10.1186/s13662-021-03438-1.
[14] S. Cipolla, F. Durastante, and F. Tudisco, *Nonlocal pagerank*, ESAIM Math. Model. Numer. Anal. 55 (2021), pp. 77–97. Available at https://doi.org/10.1051/m2an/2020071. MR 4216832.
[15] E.A. Coddington and N. Levinson, *Theory of Ordinary Differential Equations*, McGraw-Hill Book Co. Inc., New York-Toronto-London, 1955.
[16] W.A. Coppel, *Dichotomies in Stability Theory*, Lecture Notes in Mathematics, Vol. 629, Springer-Verlag, Berlin-New York, 1978. MR 0481196.
[17] E. Estrada, *Path laplacian matrices: Introduction and application to the analysis of consensus in networks*, Linear Algebra Appl. 436 (2012), pp. 3373–3391. Available at https://doi.org/10.1016/j.laa.2011.11.032. MR 2900722.
[18] E. Estrada, *Path laplacians versus fractional Laplacians as nonlocal operators on networks*, New J. Phys. 23 (2021), p. 073049. Available at https://doi.org/10.1088/1367-2630/ac14ac. MR 4347094.
[19] E. Estrada, J.C. Delvenne, N. Hatano, J.L. Mateos, R. Metzler, A.P. Riascos, and M.T. Schaub, *Random multi-Hopper model: Super-fast random walks on graphs*, J. Complex Netw. 6 (2018), pp. 382–403. Available at https://doi.org/10.1093/comnet/cnx043. MR 3815191.
[20] E. Estrada, E. Hameed, N. Hatano, and M. Langer, *Path Laplacian operators and superdiffusive processes on graphs. I. One-dimensional case*, Linear Algebra Appl. 523 (2017), pp. 307–334. Available at https://doi.org/10.1016/j.laa.2017.02.027. MR 3624678.
[21] E. Estrada, E. Hameed, M. Langer, and A. Puchalska, *Path Laplacian operators and superdiffusive processes on graphs. II. Two-dimensional lattice*, Linear Algebra Appl. 555 (2018), pp. 373–397. Available at https://doi.org/10.1016/j.laa.2018.06.026. MR 3834211.
[22] R. Garrappa, A. Giusti, and F. Mainardi, *Variable-order fractional calculus: A change of perspective*, Commun. Nonlinear Sci. Numer. Simul. 102 (2021), p. 105904. Available at https://doi.org/10.1016/j.cnsns.2021.105904. MR 4268683.
[23] J.K. Hale, *Ordinary Differential Equations*, 2nd ed., Robert E. Krieger Publishing Co., Inc., Huntington, 1980.
[24] S. Harizanov, R. Lazarov, S. Margenov, and P. Marinov, *Numerical solution of fractional diffusion–reaction problems based on BURA*, Comput. Math. Appl. 80 (2020), pp. 316–331. Available at https://doi.org/10.1016/j.camwa.2019.07.002. MR 4099859.
[25] N.J. Higham, *Functions of Matrices: Theory and Computation*, Society for Industrial and Applied Mathematics (SIAM), Philadelphia, 2008.
[26] Y. Huang and A. Oberman, *Numerical methods for the fractional Laplacian: A finite difference-quadrature approach*, SIAM J. Numer. Anal. 52 (2014), pp. 3056–3084. Available at https://doi.org/10.1137/140954040. MR 3504596.
[27] J.D. Lambert, *Numerical Methods for Ordinary Differential Systems: The Initial Value Problem*, John Wiley & Sons, Ltd., Chichester, 1991.
[28] S. Massei and L. Robol, *Rational Krylov for Stieltjes matrix functions: Convergence and pole selection*, BIT 61 (2021), pp. 237–273. Available at https://doi.org/10.1007/s10543-020-00826-z. MR 4235307.
[29] I. Moret and P. Novati, *Krylov subspace methods for functions of fractional differential operators*, Math. Comp. 88 (2019), pp. 293–312. Available at https://doi.org/10.1090/mcom/3332. MR 3854059.

[30] G. Rajchakit, R. Sriraman, N. Boonsatit, P. Hammachukiattikul, C.P. Lim, and P. Agarwal, *Exponential stability in the Lagrange sense for Clifford-valued recurrent neural networks with time delays*, Adv. Differ. Equations 2021 (2021), p. 256. Available at https://doi.org/10.1186/s13662-021-03415-8.
[31] G. Rajchakit, R. Sriraman, N. Boonsatit, P. Hammachukiattikul, C.P. Lim, and P. Agarwal, *Global exponential stability of Clifford-valued neural networks with time-varying delays and impulsive effects*, Adv. Differ. Equations 2021 (2021), p. 208. Available at https://doi.org/10.1186/s13662-021-03367-z.
[32] G. Rajchakit, P. Agarwal, and S. Ramalingam, *Stability Analysis of Neural Networks*, Springer, Singapore, 2021.
[33] A.P. Riascos and J.L. Mateos, *Fractional dynamics on networks: Emergence of anomalous diffusion and Lévy flights*, Phys. Rev. E 90 (2014), p. 032809. Available at https://link.aps.org/doi/10.1103/PhysRevE.90.032809
[34] A.P. Riascos, T.M. Michelitsch, and A. Pizarro-Medina, *Nonlocal biased random walks and fractional transport on directed networks*, Phys. Rev. E 102 (2020), p. 022142. Available at https://link.aps.org/doi/10.1103/PhysRevE.102.022142.
[35] R.A. Rossi and N.K. Ahmed, *The Network Data Repository with Interactive Graph Analytics and Visualization*, Proceedings of the Twenty-Ninth AAAI Conference on Artificial Intelligence. The AAAI Press: Palo Alto, California; 2015.
[36] S. Samko, *Fractional integration and differentiation of variable order: An overview*, Nonlinear Dynam.71 (2013), pp. 653–662. Available at https://doi.org/10.1007/s11071-012-0485-0. MR 3030128.
[37] L. Šubelj and M. Bajec, *Robust network community detection using balanced propagation*, The Eur. Phys. J. B 81 (2011), pp. 353–362. Available at https://doi.org/10.1140/epjb/e2011-10979-2.
[38] A. van Heukelum, G. Barkema, and R. Bisseling, *DNA electrophoresis studied with the cage model*, J. Comput. Phys. 180 (2002), pp. 313–326. Available at https://www.sciencedirect.com/science/article/pii/S0021999102970956.
[39] M.Y. Wu, *A note on stability of linear time-varying systems*, IEEE Trans. Automatic Control AC-19 (1974), p. 162. Available at https://doi.org/10.1109/tac.1974.1100529. MR 0393692.
[40] P. Zhuang, F. Liu, V. Anh, and I. Turner, *Numerical methods for the variable-order fractional advection–diffusion equation with a nonlinear source term*, SIAM J. Numer. Anal. 47 (2009), pp. 1760–1781. Available at https://doi.org/10.1137/080730597. MR 2505873.